Nanoscale

RSC Publishing

PAPER

View Article Online
View Journal

Paramagnetic nanoparticles to track and quantify *in vivo* immune human therapeutic cells

Cite this: DOI: 10.1039/c3nr34240a

Caroline Aspord,[ab] David Laurin,[ab] Marc F. Janier,[cde] Céline A. Mandon,[cf] Charles Thivolet,[cdg] Christian Villiers,[bh] Pierre Mowat,[ce] Anne-Marie Madec,[cg] Olivier Tillement,[ce] Pascal Perriat,[i] Cédric Louis,[j] Frédéric Bérard,[cdk] Patrice N. Marche,[bh] Joël Plumas[ab] and Claire Billotey†*[cde]

This study aims to investigate gadolinium-based nanoparticles (Gd-HNP) for *in vitro* labeling of human plasmacytoid dendritic cells (HuPDC) to allow for *in vivo* tracking and HuPDC quantifying using magnetic resonance imaging (MRI) following parenteral injection. Human plasmacytoid DC were labeled (LabHuPDC) with fluorescent Gd-HNP (Gd-FITC-HNP) and injected *via* intraperitoneal and intravenous routes in 4–5 NOD-SCID $\beta 2m^{-/-}$ mice (treated mice = TM). Control mice (CM) were similarly injected with unlabeled HuPDC. *In vivo* 7 T MRI was performed 24 h later and all spleens were removed in order to measure Gd and fluorescence contents and identify HuPDC. Gd-FITC-HNP efficiently labeled HuPDC (0.05 to 0.1 pg per cell), without altering viability and activation properties. The magnetic resonance (MR) signal was exclusively due to HuPDC. The normalized MR splenic intensity for TM was significantly higher than for CM ($p < 0.024$), and highly correlated with the spleen Gd content ($r = 0.97$), and the number of HuPDC found in the spleen ($r = 0.94$). Gd-FITC-HNP allowed for *in vivo* tracking and HuPDC quantifying by means of MRI following parenteral injection, with very high sensitivity (<3000 cells per mm^3). The safety of these new nanoparticle types must be confirmed *via* extensive toxicology tests including *in vivo* stability and biodistribution studies.

Received 21st December 2012
Accepted 17th June 2013

DOI: 10.1039/c3nr34240a

www.rsc.org/nanoscale

Introduction

In December 2011, a total of 20 808 clinical trials using cellular therapy were registered in the United States.[1] A major potential application of these therapies is cancer treatment using dendritic cell (DC) vaccinations or antigen-specific T-cell transfer. Since the first clinical trial using DC[2]-based immunotherapy in 1996, many teams have been working towards improving the efficacy of these therapies.

Since 1999, radiolabeling of DC with ^{111}In-oxinate[3] allowed the relevance of the administration route (sub-cutaneous or intra-dermic) to be demonstrated *in vivo* in humans, thereby enabling DC to reach the lymph nodes and causing anti-tumor activity. However, due to low spatial resolution, *ex vivo* analysis by auto-radiography was necessary to demonstrate the intra-nodal-localization of DC.

To overcome this method's limitations, the authors proposed, in 2005 (ref. 4) to combine magnetic resonance imaging (MRI) and scintigraphy imaging using co-injection of DC labeled with either ^{111}In-oxinate or iron-oxide particles. This approach proved, however, unsatisfactory, due to its lack of sensitivity and the absence of proportionality between the signal detected and the number of cells. The experts' efforts led to the development of other agents for cellular labeling, namely fluorine agents,[5] which required specific sequences and tools for MRI detection.

Other teams[6] developed cell labeling nanoprobes based on gadolinium (Gd). A Gd-nanoprobe exhibits the advantage of enhancing the MRI signal and of providing a signal proportional to Gd-nanoprobe concentration. *In vitro* studies[5] confirmed the higher sensitivity obtained with these agents in comparison to iron oxide particles. Nevertheless, no *in vivo* study using Gd-nanoprobe and focusing on therapeutic human cell monitoring has yet been published.

Our consortium has developed gadolinium oxide-based nanoparticles (Gd-FITC-HNP) that generate a highly enhanced MRI signal,[7] with elevated cellular internalization.[8]

[a]*R&D Laboratory, Etablissement Français du Sang Rhône Alpes, La Tronche, F-38701 France*
[b]*Université Joseph Fourier, UMR 823, Grenoble, France*
[c]*Université Claude Bernard Lyon1, France*
[d]*Hospices Civils de Lyon, Lyon, France*
[e]*Laboratoire LPCML UMR5620, Villeurbanne, France*
[f]*Laboratoire CREATIS-LRMN UMR 5220 UCBL-CNRS, France*
[g]*INSERM U870, Faculté de Médecine Lyon-sud, Pierre-Bénite, France*
[h]*INSERM U823, Institut Albert Bonniot, La Tronche, F-38706 France*
[i]*INSA de Lyon – Laboratoire MATEIS, Villeurbanne, France*
[j]*Société Nano-h, Saint-Quentin Fallavier, France*
[k]*INSERM U851, Lyon, France*
† Corresponding address: Service de Médecine Nucléaire, Hôpital, Nord – CHU Saint-Etienne, Avenue Albert Raimond, 42270 Saint-Priest-en-Jarez, France. E-mail: claire.billotey@chu-st-etienne.fr

This study aims to demonstrate the feasibility of detecting and quantifying, using *in vivo* MRI, the presence of labeled human therapeutic cells, following intravenous (IV) and intraperitoneal injection (IP) of gadolinium oxide-based nanoparticles.

Methods

Oxide gadolinium-FITC-hybrid nanoparticles (Gd-FITC-HNP)

The hybrid multimodal core–shell nanoparticles were synthesized in a three-step route. A transparent colloidal solution in DEG of 3.5 nm Gd_2O_3 cores was obtained by adding, at room temperature, a sodium hydroxide solution to gadolinium trichloride (Nano-H SAS, Saint-Quentin Fallavier, France).[9] The polysiloxane shell growth was achieved by sequential addition of tetraethyl orthosilicate and aminopropyl triethoxysilane (APTES) (in a 40/60 ratio) (Aldrich Chemical, Saint-Quentin Fallavier, France). Prior to this step, fluorescein isothiocyanate (FITC) (Aldrich Chemical, Saint-Quentin Fallavier, France) was covalently linked to an APTES part in order to obtain a fluorescent polysiloxane shell,[7] producing nanoparticles of about 5 nm. Covalent diethylenetriaminepentaacetic acid grafting was carried out by adding diethylenetriaminepentaacetic acid bisanhydride (Chematch, Dijon, France) dissolved in anhydrous dimethyl sulfoxide (Aldrich Chemical, Saint-Quentin Fallavier, France). Purification was achieved by precipitation in acetone and high-rate tangential centrifugation in water (5 kDa membrane; purification ratio >1/1000). The Gd-FITC-HNP longitudinal and transversal relaxation rates were 11.3 and 14.7 s^{-1} mM^{-1}, respectively, at 600 MHz and 37 °C.

Human plasmacytoid dendritic cells (HuPDC)

HuPDC were obtained from a pDC cell line, as previously described;[10] anti-human CD45, CD123, CD40 Abs, and 7AAD markers were purchased from Beckman Coulter (Marseille, France). Anti-HLA Class I and CD86 Abs were purchased from BD (Claix, France).

Cell labeling

HuPDC were washed in *phosphate buffered saline* resuspended at 10×10^6 cells per mL, and incubated for 1 h at room temperature with Gd-FITC-HNP at 0, 5, or 10 mM equivalent gadolinium concentrations. HuPDC were washed three times prior to further use. Cell viability was assessed by flow cytometry using 7AAD labeling at 0, 4, and 24 h after the labeling process. The percentage of labeled cells was evaluated by measuring the FITC signal. Confocal microscopy was performed at 0, 4, and 24 h after cell labeling using a spectral TCS-SP2 Leica instrument in order to investigate Gd-FITC-HNP location in HuPDC. For functional tests, HuPDC were resuspended at 2×10^6 cells per mL in Roswell Park Memorial Institute medium (RPMI) 10% fetal calf serum and stimulated for 24 hours with either 640 hemagglutinating formaldehyde unit per mL inactivated influenza virus (strain A/H3N2/Wisconsin/67/05, Sanofi Pasteur, Marcy-L'étoile, France) FCS (Gibco) or 10 μg mL^{-1} CpG_A ODN 2336 (TLR9-L; Coley Pharmaceuticals, Berlin, Germany). Cell activation was measured by labeling HuPDC with anti-HLA Class I, -CD40, and -CD86 Abs and through analysis on a FACSCalibur flow cytometer (BD, Claix, France). Culture supernatants were tested for IFNα, TNFα, and IP10 using a Cytometric Bead Array multiplex (BD, Claix, France). To evaluate the MR signal provided by labeled HuPDC, agarose phantoms were performed containing 10^6 per mL of 5 mM-Gd-HNP labeled HuPDC and the same amount of unlabeled HuPDC, with simultaneous MR imaging at 7 T with a MR Biospec™ system (Brüker, Wissenbourg, France) equipped with 400 mT m^{-1} gradient using T1w sequences (MSME sequence, [repetition time ms/echo time ms] = 200/11, flip angle = 180°, and 256 × 128 matrix). Enhancement of contrast (EHC) between labeled and unlabeled cells was defined as (signal of the labeled sample − signal of the unlabeled sample)/signal of the unlabeled sample.

In vivo studies

Tested animals were NOD-SCID $\beta 2m^{-/-}$ immunodeficient mice (NOD.Cg-Prkdc^{SCID}β2m^{Tm1Unc}/J) purchased from Jackson ImmunoResearch Laboratories (Marseille, France) and bred at Plateforme de Haute Technologie Animale (Grenoble, France). All *in vivo* experiments were approved by the local animal ethic committees. Two different routes of injection were used, IP (experiment #1 conducted in 10 mice including 5 controls) and IV (experiment #2 conducted in 9 mice, including 5 controls). As the homing of HuPDC following intraperitoneal and intravenous injection was exclusively limited to the spleen, with exception of the lymph nodes (data of biodistribution study performed after ^{111}In-oxinate labeling of HuPDC not shown), MR imaging was focused on the spleen. Twenty (experiment #2) to 30 (experiment #1) million HuPDC were injected per mouse, labeled with Gd-FITC-HNP at 10 mM equivalent gadolinium concentration and unlabeled (control). Measurement of metal Gd content in labeled cell pellets was performed using inductively plasma-mass spectrometry (ICP-MS) (Ascal, Forbach, France); mean Gd content per HuPDC was estimated as the ratio of total Gd content to the number of HuPDC in the cell pellets.

All mice, except the one that died during anesthesia, were imaged for 12 to 24 h following HuPDC injection using a 7 T MR Biospec™ system (Brüker, Wissenbourg, France) equipped with 400 mT m^{-1} gradient under gaseous anesthesia (Isoflurane®, Laboratoire Belamont, Neuilly-sur-Seine, France). The imaging protocol consisted of a series of 12 transaxial slices centered on the spleen area and obtained using inversion-recovery prepared T_1-weighed gradient echo sequences including a black blood modulus (191/2.4 [repetition time ms/echo time ms], inversion time = 50 ms, flip angle = 70°, 0.75 mm section thickness, 30 mm field of view, and 256–256 matrix). Acquisitions were triggered on respiration (Rapid Biomedical GmbH).

The spleen and background region of interest (ROI) were drawn on axial images centered on the spleen, and the signal was measured and normalized by dividing the spleen value by the standard deviation (SD) of the background signal. Normalized spleen values between the two groups were compared in both *in vivo* experiments using unpaired two-tailed tests.

The presence of HuPDC was determined using one half of the spleen to measure the percentage of $hCD45^+$ $hCD123^+$ cells by flow cytometry, and the mean fluorescence intensity of FITC was quantified in the $hCD45^+$ $hCD123^+$ fraction. The other half of the spleen, with one exception in experiment #2 (due to technical problems), was used to measure Gd concentration by ICP-MS. The number of labeled HuPDC in the spleen was estimated by dividing the Gd mass contained in the spleen by the mean Gd content per HuPDC. The normalized MRI spleen signal intensity correlated with the spleen Gd content and mean labeled HuPDC in the spleen. The number of labeled cells detected *via* MRI per unit of volume was estimated using the mean spleen volume of 3 mice (according to the ellipsoid volume formula $V = 4/3\ \pi abc$, with length $= 2a$, width $= 2b$, and thickness $= 2c$).

Results

Labeling of human plasmacytoid dendritic cells (HuPDC) with Gd-FITC-HNP

Gd-FITC-HNP were efficiently taken up by and internalized in HuPDC, as shown by confocal analysis (Fig. 1a). The mean fluorescence intensity (MFI) value demonstrated a better internalization at 10 mM, than at 5 mM for Gd equivalent concentration in the incubation media (Fig. 1b). Mean Gd content per cell was estimated at 0.05 to 0.1 pg after incubation at 10 mM. Labeling efficiency of HuPDC with Gd-FITC-HNP at 10 mM was excellent, since >98% of cells were labeled (Fig. 1c). No evidence of toxicity was observed using 7AAD staining of dead cells after incubation at 10 mM for 24 h (Fig. 2a and b).

Functional tests of labeled HuPDC

The labeling process with Gd-FITC-HNP at 10 mM of Gd equivalent concentration did not induce HuPDC activation, since similar expression levels were measured for costimulatory molecules and cytokine secretion as compared to control conditions (Fig. 3a).

The labeling did not alter the HuPDC activation process in response to TLR-L stimulation. Indeed, the following was observed: (i) similar expression levels of HLA Class I and co-stimulatory molecules by labeled and unlabeled HuPDC following stimulation by TLR-L (Fig. 3b and c); (ii) similar

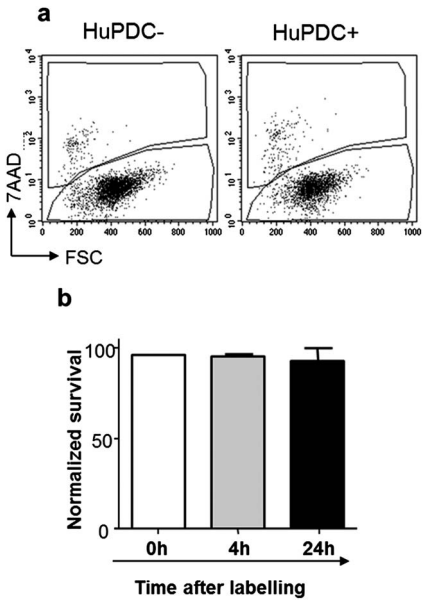

Fig. 2 Evaluation of *in vitro* functionality of labeled HuPDC. (a) Viability analysis by flow cytometry of human dendritic cells labeled with Gd-FITC-HNP; viable cells are 7AAD negative. One representative experiment is shown. (b) Normalized survival of human dendritic cells after labeling with 5–10 mM Gd-FITC-HNP immediately after, at 4 h and 24 h following the labeling process (data from eight independent experiments).

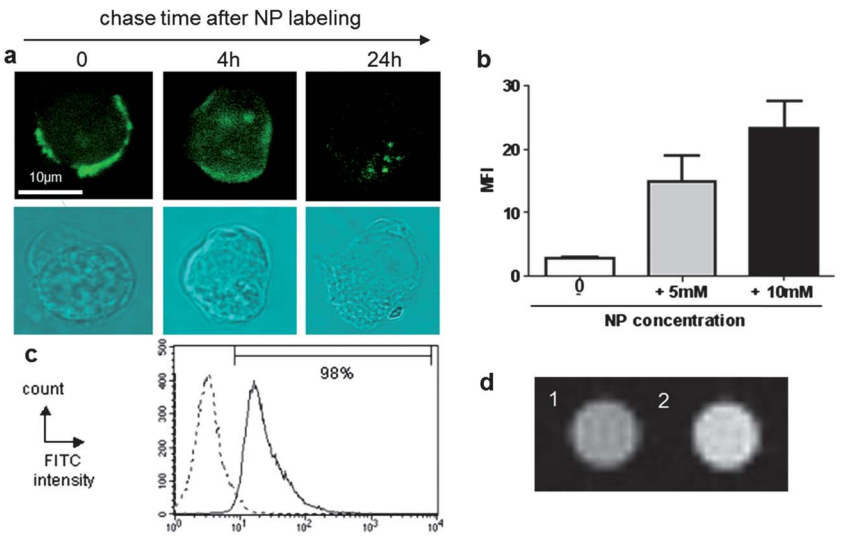

Fig. 1 Evaluation of HuPDC labeling efficiency with Gd-FITC-HNP. (a) Confocal imaging of human dendritic cells immediately after and at 4 and 24 h following labeling with Gd-FITC-HNP. (b) FITC signal intensity (MFI) of nanoparticle-labeled human dendritic cells at 5 mM and 10 mM (data from eight independent experiments). (c) FITC signal intensity (MFI) of unlabeled (discontinuous line) and Gd-FITC-HNP labeled (continuous line) HuPDC. (d) T_1-weighted MR images of agarose phantoms containing 10^6 per mL of unlabeled (1) and Gd-HNP labeled (2) HuPDC. The EHC (1 *vs.* 2) was calculated at 33%.

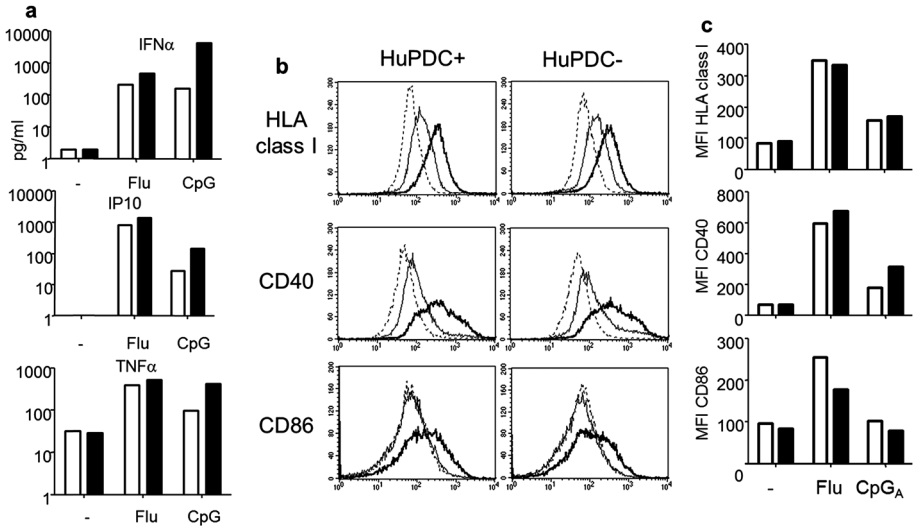

Fig. 3 Verification of the absence of HuPDC activation due to the labeling process and the intact ability of activation of labeled HuPDC. HuPDC were labeled or not labeled with 10 mM Gd-FITC-HNP and then stimulated with TLR7 (Flu) and TLR9 (CpG_A) ligands. (a and b) Flow cytometric analysis of HLA Class I and costimulatory molecules CD40 and CD86 24 h after activation. (a) Dotted line: unstimulated cells; plain line: TLR9-L stimulation; bold line: TLR7-L stimulation. (b) White bars: unlabeled and black bars: Gd-FITC-HNP labeled cells. (c) Cytokine secretion analysis in the supernatants 24 h after cell activation by a cytometric beads array. White bars: unlabeled cells and black bars: Gd-FITC-HNP labeled cells.

capacity to produce IFNα, TNFα, and IP10 cytokines following TLR7-L (Flu virus) and TLR9-L (CpG_A) activation in the labeled HuPDC population as opposed to the unlabeled one (Fig. 3a). Efficacy of 5 mM Gd-HNP labeled cells on the MR signal was visually detected and proven by EHC estimated at 33%.

In vivo MRI

On visual analysis, the spleen MR signal appeared brighter in mice injected with labeled HuPDC compared to control mice, whether by IP or IV injection (Fig. 4). The normalized mean spleen signal in mice injected with labeled HuPDC was significantly higher than in control mice ($p \leq 0.0003$ and $p = 0.024$ in experiments 1 and 2, respectively) (Fig. 5a). The normalized mean spleen signal correlated with whole spleen Gd content ($r = 0.97$) (Fig. 5b).

Harvested spleen analysis by flow cytometry demonstrated that fluorescence detected FITC, related to Gd-FITC-HNP, corresponded uniquely to HuPDC contingent, characterized by co-expression of hCD45 and hCD123 markers (Fig. 6a and c). The contingent's fluorescence was identical to that of the other spleen cells in the unlabeled HuPDC-injected mice. The significantly higher MR signal value in the spleen of labeled cell-injected mice was thus correlated with injected HuPDC in the spleen, and not with indirect macrophage labeling. HuPDC were found in similar quantities in the spleen of unlabeled-injected and labeled-injected mice (Fig. 6a and b). Therefore, labeling was stable *in vivo* without altering HuPDC functionality, as they were able to quickly migrate into the spleen closely following injection.

The number of labeled HuPDC in the spleen was calculated as the ratio of spleen Gd content to Gd content per cell, and was found to be lower after IP (ranging from 6×10^4 to 1.8×10^5 – mean $\pm$ SD $= 9.85 \times 10^4 \pm 5.1 \times 10^4$) than IV injection (ranging from 2.8 to 3.38×10^5 – mean $\pm$ SD $= 2.92 \times 10^5 \pm 3.34 \times 10^4$). Sixty thousand cells labeled with Gd-FITC-HNP were detected in the spleen, with an average volume estimated to be 22.5 mm^3. Therefore, the number of labeled cells detected *in vivo* by MRI was approximately 2667 cells per mm^3, or 33.2 cells per voxel (volume = 0.01246 mm^3). The normalized mean spleen signal correlated with the labeled cell number localized in the spleen ($r = 0.94$).

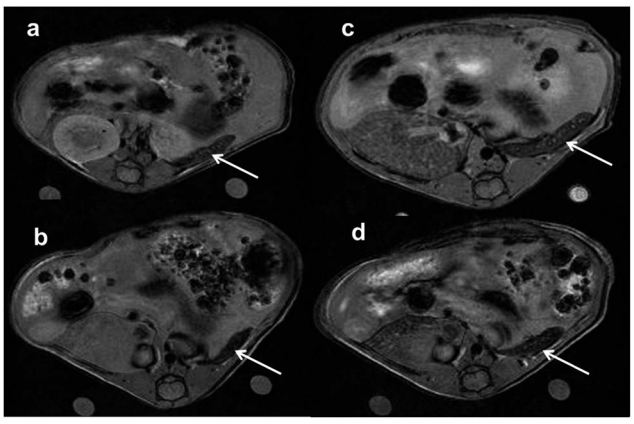

Fig. 4 Representative MR imaging performed in 4 mice injected with unlabeled and labeled HuPDC. Axial MRI views centered on spleen area (arrows) acquired in four representative mice injected using IP (a and b) and IV (c and d) routes, after injection of labeled (a and c) and unlabeled (b and d) HuPDC. The normalized signal in the spleen was measured in mice at 19.2, 11.9, 33.7, and 20.4, respectively in a, b, c and d. The Gd content was undetectable in the spleen of the (b) and (d) mice, and measured at 17.6 and 34.6 ng in the spleen (a) and (c), respectively, with an estimated number of labeled HuPDC of 1.78×10^5 and 3.38×10^6, respectively.

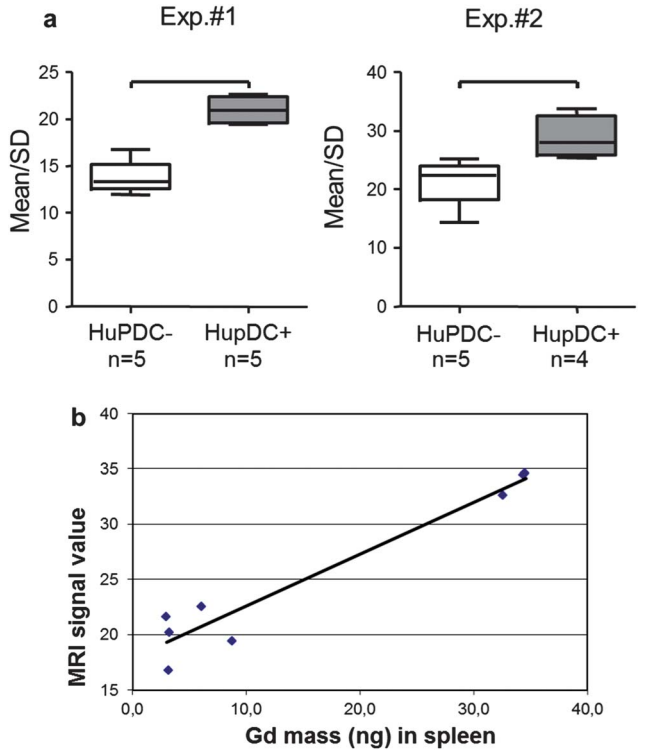

Fig. 5 Statistical analysis of quantitative MRI and Gd spleen content data. Graph (a) presents the normalized MRI signal in the spleen of mice injected with unlabeled (HuPDC−) and labeled HuPDC (HuPDC+) in experiments 1 and 2. The values in HuPDC+ groups were higher than and significantly different from controls ($p \leq 0.0003$ and 0.024 in experiments 1 and 2, respectively). Graph (b) presents the correlation between the MRI normalized signal in the spleen of mice injected with labeled HuPDC and the Gd content (expressed in ng) in the spleen at 0.96.

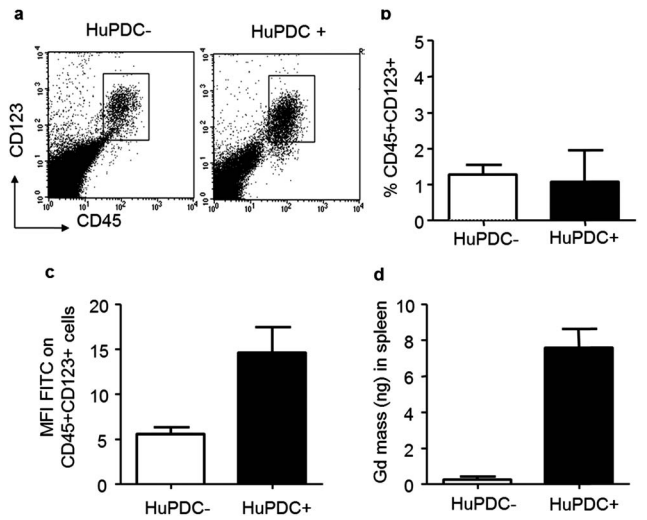

Fig. 6 Flow cytometry analysis of harvested spleen removed at 24 hours after injection of labeled and unlabeled HuPDC. (a and b) *Ex vivo* detection of human dendritic cells by flow cytometry within the spleen of injected animals using hCD45 and hCD123 HuPDC markers. (a) A representative mouse of each experimental group is shown. (b) Percentages of human pDC detected in the spleen of animals for each group. (c) FITC signal intensity (MFI) on $CD45^+$ $CD123^+$ human pDC (6 animals for each group). (d) Gd dosage of the spleen by ICP.

Discussion

We have demonstrated that human DC can be efficiently labeled with Gd-FITC-HNP, without altering *in vivo* survival, function, and homing following parenteral injection. Gd-based nanoprobes provided a positive contrast on imaging, along with elevated detection sensitivity, and proportionality between the signal measured and the labeling agent quantity, in other words the number of labeled cells present.

Numerous experimental studies, as well as human studies,[4] have shown that iron oxide nanoparticles (IONP) allowed for the *in vivo* localization of therapeutic cells using MRI. The presence of labeled cells appears in the form of a dark spot on T_2*-weighted sequences due to magnetic field inhomogeneities caused by the presence of IONP, which increase with the magnetic field. Considering IONP's safety and given that IONP's iron incorporated in macrophagic cells is totally biodegraded,[11] several IONP types have received regulatory approval for hepatic tumor imaging (Resovist® and Teslacan®) following the parenteral route, with numerous clinical trials in *in vivo* cell trafficking having already been conducted.[1] To circumvent the difficulties in quantifying the signal due to a T_2* effect, the de Vries group also carried out scintigraphy using ^{111}In labeling in order to estimate the proportion of injected cells migrating to the lymph nodes.[12]

Recent developments allowed Gd-based complexes presenting cell internalization properties to be designed with optimized R_1 relaxation effects.[6] The positive contrast-induced changes in R_1 are easy to detect. Consequently, contrast agents with T_1-weighted enhancement should allow us to track labeled cells in low-signal tissues. Previous studies showed that the Gd nanocomplex-labeled murine stem[13] or tumoral[14] cells could be detected *ex vivo* or *in vivo*[14] using MRI after the cells' *in situ* injection. In 2005,[15] another alternative was proposed using fluoride labeling agents to perform resonance imaging of ^{19}F spectroscopy coupled with ^{1}H MRI. The objective was to free the ^{1}H background signal arising from mobile water molecules in order to increase labeled cell detection sensitivity and thus optimize MR sensitivity. The ^{19}F MR requires specific equipment (^{1}H/^{19}F double-tuned coil) to allow for superimposing anatomical data given by ^{1}H T_1-weighted sequences and ^{19}F spin-density-weighted images, thereby providing information about the presence and density of labeled cells. The entire acquisition process requires 30 minutes (ref. 5) as opposed to the 3 minutes required in our study.

To investigate the feasibility of using therapeutic human cells labeled with Gd NP for *in vivo* MRI follow-up, we used plasmacytoid dendritic cells (pDCs) injected in immunodeficient mice. These pDCs loaded with peptides derived from tumor antigens are used as an anti-tumor vaccine.[16] The detected MRI signal in the spleen is directly linked with the amount of therapeutic cells previously labeled with fluorescent Gd-FITC-HNP and not with macrophages in the mouse, which would have internalized the Gd-FITC-HNP from dead labeled HuPDC. This observation is based on the colocalization study results where all the fluorescent cells of the spleen were first recovered, in other words all the Gd-FITC-HNP containing

cells. As these cells expressed human cell markers, they were indeed the injected HuPDC.

As a previous study[17] and personal data (not shown) have indicated a larger DC accumulation in the spleen following IV compared with IP, our experiment used both routes. We obtained a large range of cell homing in the spleen, and were thus able to demonstrate a relationship between labeled cell numbers and the MRI signal intensity. This observation is of paramount importance as it paves the way for quantification, assuming mean Gd cell content is known.

In this study, we used hybrid Gd-based nanoparticles, which display a large effect on the MRI signal as seen *via* the R_1 measurement. Using a simple and rapid labeling process, we showed that, despite low Gd cell content (0.05 to 0.1 pg per cell), *in vivo* MRI cell detection was efficient with high sensitivity, as less than 3000 cells per mm^3 were detected. Given that the signal detected with contrast agents using 3 T and T_1-weighted images was at least as significant as with 7 T, the sensitivity found in our study was seen to be similar to that obtained with IONP labeled DC (2451 DC per mm^3 at 3 T after a mean loading of 30 $\pm$ 4 pg of iron per cell (ref. 4)). In contrast, the sensitivity of DC detection when using the fluorine agent appeared notably lower[5] (7.5×10^5 cells per mm^3, this estimation has been made assuming a mean inguinal node volume of 4 mm^3 in mouse). For clinical studies using 1.5 or 3 T MRI, we expect to achieve at least the same sensitivity as the one reported here, given that longitudinal relaxation increases as the intensity of the magnetic field decreases,[18] especially at 1.5 T.[19]

To translate these findings into clinical applications, which will likely inject 6 to 90 millions of HuPDC, and assuming that only 2 (ref. 17) to 4% (ref. 12) of HuPDC will migrate to lymph nodes (volume estimated at 65 mm^3), the sensitivity achieved here would be sufficient for detecting and quantifying the HuPDC in lymph nodes.

Our study demonstrated labeling stability over 24 h. No data are available beyond this time period. However, *in vitro*[8] tests using human fibroblasts indicated labeling stability over 3 days. When excluding cells with elevated division rates, the proposed method allows for *in vivo* monitoring of cellular traffic over a minimum of a few days.

Conclusion

By overcoming the technological limitations (positivity of the signal generated, high sensitivity, and quantification of cells with high-resolution anatomical data), our method likely proves a powerful imaging tool to evaluate cellular therapies. This method could also be used in investigating and diagnosing at an early stage pathological human conditions, such as Type 1 diabetes *via* the direct labeling and injection of autologous T-cells. However, in contrast to IONP, Gd-based nanoparticles have not yet received regulatory approval for human use. The safety of these new nanoparticle types must be confirmed *via* extensive toxicology tests including *in vivo* stability and biodistribution studies.

Acknowledgements

This work was supported by grants from *Cancéropôle Lyon Auvergne Rhône-Alpes*. We would like to thank Aurélie BERNIARD and Jean-Baptiste LANGLOIS for their technical support, and CERMEP – Imagerie du Vivant (dedicated MRI platform access).

References

1 http://clinicaltrials.gov/ct2/results?term=cell+therapies.
2 F. J. Hsu, C. Benike, F. Fagnoni, T. M. Liles, D. Czerwinski, B. Taidi, E. G. Engleman and R. Lev, *Nat. Med.*, 1996, **2**(1), 52–58.
3 (*a*) M. A. Morse, R. E. Coleman, G. Akabani, N. Niehaus, D. Coleman and H. K. Lyerly, *Cancer Res.*, 1999, **59**(1), 56–58; (*b*) A. Mackensen, T. Krause, U. Blum, P. Uhrmeister, R. Mertelsmann and A. Lindemann, *Cancer Immunol. Immunother.*, 1999, **48**, 118–122.
4 I. J. de Vries, W. J. Lesterhuis, J. O. Barentsz, P. Verdijk, J. H. vanKrieken, O. C. Boerman, W. J. Oyen, J. J. Bonenkamp, J. B. Boezeman, G. J. Adema, J. W. Bulte, T. W. Scheenen, C. J. Punt, A. Heerschap and C. G. Figdor, *Nat. Biotechnol.*, 2005, **23**, 1407–1413.
5 F. Bonetto, M. Srinivas, A. Heerschap, R. Mailliard, E. T. Ahrens, C. G. Figdor and I. J. de Vries, *Int. J. Cancer*, 2011, **129**, 365–373.
6 (*a*) M. Modo, D. Cash, K. Mellodew, S. C. Williams, S. E. Fraser, T. J. Meade, J. Price and H. Hodges, *NeuroImage*, 2002, **17**, 803–811; (*b*) K. Vuu, J. Xie, M. A. McDonald, M. Bernardo, F. Hunter, Y. Zhang, K. Li, M. Bednarski and S. Guccione, *Bioconjugate Chem.*, 2005, **16**, 995–999; (*c*) M. Oliver, A. Ahmad, N. Kamaly, E. Perouzel, A. Caussin, M. Keller, A. Herlihy, J. Bell, A. D. Miller and M. R. Jorgensen, *Org. Biomol. Chem.*, 2006, **4**, 3489–3497; (*d*) A. Klasson, M. Ahrén, E. Hellqvist, F. Söderlind, A. Rosén, P. O. Käll, K. Uvdal and M. Engström, *Contrast Media Mol. Imaging*, 2008, **3**, 106–111; (*e*) G. Digilio, V. Catanzaro, F. Fedeli, E. Gianolio, V. Menchise, R. Napolitano, C. Gringeri and S. Aime, *Chem. Commun.*, 2009, 893–895; (*f*) C. L. Tseng, I. L. Shih, L. Stobinski and F. H. Lin, *Biomaterials*, 2010, **31**, 5427–5435.
7 J. L. Bridot, A. C. Faure, S. Laurent, C. Rivière, C. Billotey, B. Hiba, M. Janier, V. Josserand, J. L. Coll, L. V. Elst, R. Muller, S. Roux, P. Perriat and O. Tillement, *J. Am. Chem. Soc.*, 2007, **129**, 5076–5084.
8 J. Fizet, C. Rivière, J. L. Bridot, N. Charvet, C. Louis, C. Billotey, M. Raccurt, G. Morel, S. Roux, P. Perriat and O. Tillement, *J. Nanosci. Nanotechnol.*, 2009, **9**, 5717–5725.
9 C. Louis, R. Bazzi, C. A. Marquette, J. L. Bridot, S. Roux, G. Ledoux, B. Mercier, L. Blum, P. Perriat and O. Tillement, *Chem. Mater.*, 2005, **17**, 1673–1682.
10 (*a*) L. Chaperot, A. Blum, O. Manches, G. Lui, J. Angel, J. P. Molens and J. Plumas, *J. Immunol.*, 2006, **176**, 248–255; (*b*) C. Aspord, J. Charles, M. T. Leccia, D. Laurin, M. J. Richard, L. Chaperot and J. Plumas, *PLoS One*, 2010, **5**, e10458.

11 R. Weissleder, D. D. Stark, B. L. Engelstad, B. R. Bacon, C. C. Compton, D. L. White, P. Jacobs and J. Lewis, *AJR, Am. J. Roentgenol.*, 1989, **152**, 167–173.
12 P. Verdijk, E. H. Aarntzen, W. J. Lesterhuis, A. C. Boullart, E. Kok, M. M. van Rossum, S. Strijk, F. Eijckeler, J. J. Bonenkamp, J. F. Jacobs, W. Blokx, J. H. Vankrieken, I. Joosten, O. C. Boerman, W. J. Oyen, G. Adema, C. J. Punt, C. G. Figdor and I. J. de Vries, *Clin. Cancer Res.*, 2009, **15**, 2531–2540.
13 M. Modo, D. Cash, K. Mellodew, S. C. Williams, S. E. Fraser, T. J. Meade, J. Price and H. Hodges, *NeuroImage*, 2002, **17**, 803–811.
14 K. Vuu, J. Xie, M. A. McDonald, M. Bernardo, F. Hunter, Y. Zhang, K. Li, M. Bednarski and S. Guccione, *Bioconjugate Chem.*, 2005, **16**, 995–999.
15 E. T. Ahrens, R. Flores, H. Xu and P. A. Morel, *Nat. Biotechnol.*, 2005, **23**, 983–987.
16 C. Aspord, J. Charles, M. T. Leccia, D. Laurin, M. J. Richard, L. Chaperot and J. Plumas, *PLoS One*, 2010, **5**, e10458.
17 A. A. Eggert, M. W. Schreurs, O. C. Boerman, W. J. Oyen, A. J. de Boer, C. J. Punt, C. G. Figdor and G. J. Adema, *Cancer Res.*, 1999, **59**, 3340–3345.
18 P. Caravan, C. T. Farrar, L. Frullano and R. Uppal, *Contrast Media Mol. Imaging*, 2009, **4**, 89–100.
19 S. W. Zielhuis, J. H. Seppenwoolde, V. A. Mateus, C. J. Bakker, G. C. Krijger, G. Storm, B. A. Zonnenberg, A. D. van het Schip, G. A. Koning and J. F. Nijsen, *Cancer Biother. Radiopharm.*, 2006, **21**, 520–527.